FEBS Letters 586 (2012) 3404–3409

journal homepage: www.FEBSLetters.org

Coilin levels modulate cell cycle progression and γH2AX levels in etoposide treated U2OS cells

Venkatramreddy Velma, Zunamys I. Carrero, Carmen B. Allen, Michael D. Hebert *

Department of Biochemistry, The University of Mississippi Medical Center, Jackson, MS 39216-4505, USA

ARTICLE INFO

Article history:
Received 30 March 2012
Revised 5 July 2012
Accepted 17 July 2012
Available online 7 August 2012

Edited by Ivan Sadowski

Keywords:
Coilin
DNA damage
Cell cycle
γH2AX

ABSTRACT

Coilin is considered the Cajal body (CB) marker protein. In this report, we investigated the role of coilin in the DNA damage response and found that coilin reduction correlated with significantly increased levels of soluble γH2AX in etoposide treated U2OS cells. Additionally, coilin levels influenced the proliferation rate and cell cycle distribution of cells exposed to etoposide. Moreover, coilin overexpression inhibited nucleolar localization of endogenous coilin in etoposide treated U2OS cells. Collectively, these data provide additional evidence for coilin and CBs in the DNA damage response.

1. Introduction

Coilin is considered the Cajal body (CB) marker protein. CBs are subnuclear domains that participate in small nuclear ribonucleoprotein (snRNP) biogenesis and are most often found in transcriptionally active cells such as neuronal and cancer cells [1–4]. Coilin knockout and knockdown experiments have demonstrated that this protein is required for CB formation, optimal cellular proliferation, and viability (in mouse and zebrafish but not in *Drosophila*) [5–10]. Considering that coilin has been shown to interact with several factors within CBs, including itself [11], it is possible that coilin plays an important role in the initial formation of this nuclear structure. Moreover, our recent work showing that coilin has both nucleic acid binding and RNase activities indicates that this protein may participate more directly in snRNA biogenesis than previously believed [12]. Mutational analysis of suspected and known coilin phosphorylation sites demonstrates that this modification impacts cellular proliferation and CB formation as well as coilin localization and stability [13–16].

Deciphering the underlying mechanisms for CB protein modification is an active area of investigation, but it is logical to conclude that the CB is responsive to a variety of cellular signals in order to coordinate snRNP biogenesis with splicing needs. One of these signals is DNA damage. A variety of different methods for inducing DNA damage, such as herpes simplex type 1 infection, UV-C and γ-irradiation exposure, or treatment with the chemotherapeutic drug cisplatin, have been shown to disrupt CBs and redistribute coilin [16–18]. In this present study, we have extended our analysis into the role of coilin in the DNA damage response by utilizing the p53 positive U2OS cell line treated with etoposide. We demonstrate here that depletion of coilin induces soluble γH2AX levels in etoposide treated U2OS cells. Changes in coilin levels correlate with alterations in cell proliferation rate in etoposide treated cells. Also, we found that coilin overexpression during treatment increases the percent of cells in the S and G2/M phases of the cell cycle. Collectively, these data further indicate a role for coilin and CBs in the DNA damage response.

2. Materials and methods

2.1. Cell culture, transfections, immunoblotting and immunofluorescence

Human osteosarcoma cells (U2OS), a gift from Dr. Luis Martinez (The University of Mississippi Medical Center, Jackson, MS), were obtained from the American Type Culture Collection (Manassas, VA). These cells were cultured using the conditions described previously [19]. GFP-tagged coilin was previously described [14,20]. DNA and duplex siRNA transfections were performed using FuGENE HD (Promega, Madison, WI) or Lipofectamine 2000 (Invitrogen, Carlsbad, CA), respectively, according to the manufacturer's specifications and as previously described [10,16]. For coilin

* Corresponding author. Address: Department of Biochemistry, The University of Mississippi Medical Center, 2500 North State Street, Jackson, MS 39216-4505, USA. Fax: +1 601 984 1501.
E-mail address: mhebert@umc.edu (M.D. Hebert).

0014-5793/$36.00
http://dx.doi.org/10.1016/j.febslet.2012.07.054

reduction, a combination of two different duplex siRNAs was employed (N004645.12.4 and the coilin 2 duplex previously published [10,16]). The duplex siRNAs were obtained from Integrated DNA Technologies (Coralville, Iowa). Cells were treated with 20 μM etoposide for 16 h unless otherwise stated. Immunofluorescence, Western blotting and image acquisition were carried out as described previously [19]. The following antibodies were used: rabbit polyclonal anti coilin (H300, Santa Cruz Biotechnology, Santa Cruz, CA), rabbit polyclonal anti-γH2AX (Bethyl, Montgomery, TX), mouse monoclonal anti-β-tubulin (Sigma–Aldrich, St. Louis, MO), mouse monoclonal anti-fibrillarin [16] and mouse monoclonal anti-GFP (Roche, Mannheim, Germany).

2.2. Soluble γH2AX protein isolation

Soluble γH2AX proteins were isolated as described previously [21] with a few modifications. Briefly, U2OS cells were lysed in 500 μl buffer A (20 mM HEPES, pH 7.9, 0.5 mM DTT, 1 mM PMSF, 1.5 mM $MgCl_2$, 0.1% Triton and 1 M NaCl) and incubated at 4 °C for 40 min and then centrifuged at 100,000 g (TL-100 Ultracentrifuge, Beckman) for 20 min. Total γH2AX proteins were obtained by sonication in RIPA buffer (50 mM Tris–HCl pH 7.6, 150 mM NaCl, 1% NP-40, 0.25% sodium deoxycholate, 0.1% SDS, 1 mM EDTA). Supernatants were subjected to SDS–PAGE, Western blotting and detection of proteins using the antibodies described above. Protein signals were quantified with Quantity One software using a Chemidoc XRS system (Biorad, Hercules, CA).

2.3. Propidium iodide staining, FACS analysis and proliferation assays

U2OS cells transfected with empty GFP vector or GFP-coilin for 24 h were untreated or treated with etoposide for an additional 16 h. The cells were then harvested and washed with PBS by centrifuging at 1500 rpm for 3 min. Each sample for FACS analysis had 0.5×10^6 cells. The cells were fixed with ice cold 70% ethanol for 30 min and washed with PBS. Cell pellets were then dissolved in 350 μl PBS and incubated with 30 μl of Ribonuclease A (10 mg/ml) (Sigma, St Louis, MO) for 5 min at room temperature. The cells were stained with 150 μl of Propidium Iodide (250 μg/ml) for 15 min at room temperature. The cell cycle distribution of GFP and GFP-coilin expressing cells was analyzed using the Gallios Flow Cytometer (Beckman Coulter) with data analysis by Kaluza software (version 1.1). For proliferation studies, U2OS cells were transfected with siRNA or plasmid DNA for 24 h, followed by seeding into a 96-well plate with 5000 cells per well [16]. Cells were untreated or etoposide treated the same day as seeding. 48 h post transfection, cell number was estimated using the cell titer blue reagent (Promega) as described in the manufacturer's protocol. The cells were read using the 490/540 filter set on FLx800 Spectrophotometer (BioTek, Winooski, VT).

3. Results

3.1. Coilin knockdown induces soluble γH2AX levels in etoposide treated U2OS cells

Previous studies have demonstrated that coilin localization is altered by DNA damage [17,18,22,16]. To explore further the role of coilin in the DNA damage response, we evaluated whether coilin levels influence the formation of γH2AX in etoposide treated U2OS cells. Etoposide is an anti-cancer drug that forms a tertiary complex with topoisomerase II, thus promoting double strand breaks and apoptosis [23]. γH2AX is not detected in untreated cells, but is found in lysate generated from etoposide treated cells (Fig. 1A). We examined two pools of γH2AX; the soluble fraction obtained by salt extraction and the total fraction obtained by sonication. The relative level of soluble γH2AX in cells subject to control siRNA transfection followed by etoposide treatment did not significantly differ compared to that observed in non-transfected etoposide treated cells. However, soluble γH2AX levels relative to tubulin were significantly higher in coilin siRNA etoposide treated cells compared to control siRNA etoposide treated cells ($p = 0.02$, $n = 3$, Fig. 1, quantitative analysis in Fig. 1B). Coilin knockdown in the absence of etoposide was not sufficient to trigger the formation of γH2AX (Supplementary Fig. 1A). Moreover, coilin reduction did not impact total γH2AX levels in the presence of etoposide (Supplementary Fig. 1A).

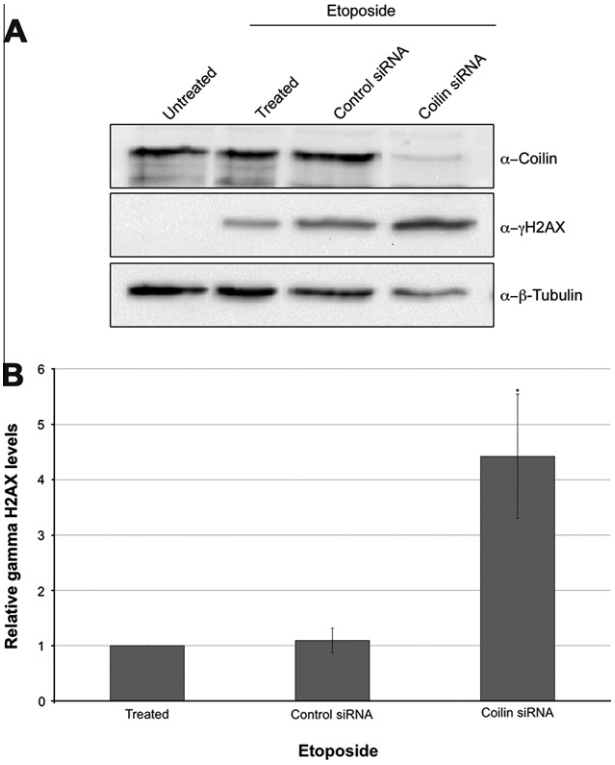

Fig. 1. Coilin reduction induces soluble γH2AX levels upon etoposide treatment. (A) U2OS cells were transfected with coilin siRNA or control siRNA for 24 h, then untreated or treated with etoposide for an additional 16 h. Cell lysates were western blotted and probed with anti-coilin (top panel), anti-γH2AX (middle panel) and anti-β tubulin antibodies (lower panel). β tubulin serves as a loading control. (B) Quantitative analysis of γH2AX relative to β-tubulin levels. The ratio of γH2AX relative to β-tubulin from treated control and coilin siRNA transfected cells were normalized to the ratio obtained from treated cells not transfected with siRNA. The increased relative γH2AX level in coilin siRNA transfected cells was statistically significant (*, $p = 0.02$, $n = 3$) compared to control siRNA γH2AX levels.

3.2. Coilin levels impact proliferation rate in cells exposed to etoposide

Previous studies have shown that coilin reduction slows cellular proliferation and attenuates decreases in proliferation associated with cisplatin treatment [9,10,16]. To examine if a similar phenotype is observed when using etoposide, we conducted proliferation assays on untreated and etoposide treated U2OS cells transfected with control or coilin siRNA (Fig. 2A). As expected, etoposide treatment reduces control siRNA transfected cell number (control KD+) by approximately 65% compared to untreated control KD (control KD). In contrast, etoposide treated coilin siRNA transfected cell number (coilin KD+) is reduced by approximately 43% compared to untreated coilin siRNA (coilin KD). Therefore, coilin knockdown diminishes the effect of etoposide and increases cell number by 22% in treated U2OS cells. In untreated cells, coilin reduction decreases cell number by approximately 35% (coilin KD compared

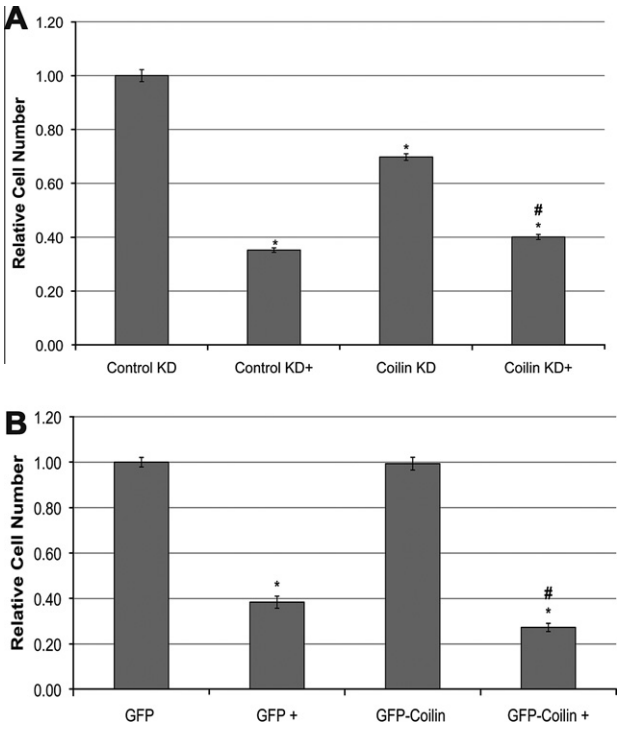

Fig. 2. Coilin impacts cell proliferation rates in etoposide treated U2OS cells. (A) Proliferation assay on U2OS cells transfected with control siRNA (control KD) or coilin siRNA (coilin KD). Data were normalized to that obtained for the untreated control KD condition (* = $p < 0.05$ versus control KD, # = $p < 0.05$ versus control KD+, n = at least 12 for each condition). (B) Proliferation assay on U2OS cells transfected with GFP or GFP-coilin and treated with etoposide (+) or untreated, normalized to the untreated GFP (GFP-coilin) transfected condition. Treated cells expressing GFP-coilin were significantly reduced in their proliferation compared to untreated or treated cells expressing GFP alone (*p = < 0.05 versus GFP, # = $p < 0.05$ versus GFP+, n = at least 12 for each condition).

to control KD), in agreement with previous results [9,10,16]. Since coilin reduction attenuated the negative effect of etoposide on proliferation compared to control siRNA, we next tested if coilin overexpression would exacerbate the decrease in proliferation as a consequence of etoposide treatment. For these studies, U2OS cells were transfected with empty GFP or GFP-coilin vectors and cell numbers were determined after treatment with etoposide or no treatment (Fig. 2B). In cells expressing GFP, cell number decreased by approximately 60% upon treatment (GFP + compared to GFP). GFP-coilin expression resulted in a more pronounced effect of etoposide, reducing cell number by approximately 75% after etoposide treatment (GFP-coilin +) compared to that obtained in the non-treated GFP-coilin expression condition (GFP-coilin), and this difference is statistically significant. The level of total or soluble γH2AX did not significantly change in GFP-coilin expressing cells compared to control (Supplementary Figs. 1B and 1C). It should be pointed out that the conditions used here (20 mM etoposide for 16 h) are not sufficient to induce apoptosis, as assessed by PARP1 cleavage (Supplementary Fig. 1D) and Annexin V staining (our unpublished observations). Collectively, these results indicate that coilin levels alter the sensitivity of cells to etoposide.

3.3. Overexpression of coilin in the presence of etoposide increases the distribution of cells in S and G2/M phases of the cell cycle

As described above, ectopically expressed coilin significantly reduces cell proliferation in etoposide treated U2OS cells (Fig. 2B). To examine if these cells have an altered cell cycle distribution, we conducted FACS analysis strictly on cells expressing GFP or GFP-coilin. Cell cycle distribution for each treatment is shown in Fig. 3. In untreated cells, GFP-coilin expression did not significantly change cell cycle distribution relative to control cells expressing GFP only. As expected, etoposide treatment of cells expressing GFP resulted in a characteristic decrease in the percent of cells in G1 and increase in the number of cells in S and G2/M. Interestingly, overexpression of coilin in treated cells further decreased the percent of cells in G1 below that found for GFP expressing cells and correspondingly increased cell distribution in S and G2/M. The differences in cell cycle distribution in the presence of etoposide between GFP and GFP-coilin expressing cells are statistically significant. These results show that reduced proliferation in the presence of etoposide as a consequence of coilin overexpression may be attributed to the accumulation of cells in S and G2/M. No significant changes in cell cycle distribution were observed in etoposide treated coilin knockdown cells (Supplementary Fig. 2).

3.4. Exogenous coilin inhibits etoposide-induced nucleolar accumulation of endogenous coilin

We have reported that DNA damaging agents redistribute coilin to the nucleolus, and depleted coilin levels increase cell viability in cisplatin treated cells [16]. We hypothesized that alteration of coilin levels would disrupt nucleolar redistribution of coilin in response to DNA damage. In a given field of untreated U2OS cells, three different coilin phenotypes can be observed (n = 100, Fig. 4A, upper panel). The majority of cells (52%) have at least 1 CB, other cells display only nucleoplasmic coilin (38%), and a sizeable fraction contain nucleolar coilin (10%). Upon exposure to etoposide, the number of cells with CBs is decreased (14%), but the percent of cells with nucleoplasmic (50%) or nucleolar localization (36%), verified by co-staining with fibrillarin, is increased (n = 100, Fig. 4AB,). Time course experiments do not detect coilin accumulation at sites of DNA damage after etoposide treatment. In order to test if coilin overexpression alters nucleolar relocalization of endogenous coilin upon etoposide treatment, U2OS cells were transfected with GFP or GFP-coilin and treated or untreated (Fig. 4C). Treated U2OS cells have the expected nucleolar localization of endogenous coilin (double arrowhead) in GFP transfected or non-transfected cells. However, GFP-coilin expression in the presence of etoposide results in different phenotypes for the endogenous coilin based on the expression level of GFP-coilin (Fig. 4C, lower panels). In treated cells with faintly detected GFP-coilin, both endogenous coilin and GFP-coilin display nucleolar accumulation (Fig. 4C, middle panel, treated, low expression). Note that since the antibody used here reacts with both GFP-coilin and endogenous coilin, it is assumed that the coilin signal represents both endogenous coilin and GFP-coilin. In contrast to that observed in etoposide-treated low expressing cells, treated cells displaying medium expression show predominantly nucleoplasmic localization of GFP-coilin and lack significant nucleolar accumulation (Fig. 4C, lower panel). These results demonstrate that exogenous coilin can act in a dominant negative manner to inhibit the nucleolar localization of endogenous coilin in the presence of etoposide.

4. Discussion

To extend previous studies demonstrating a relationship between coilin and the DNA damage response [16–18,22], we conducted experiments designed to ascertain if coilin modulates proteins involved in this pathway. For these studies, we employed the U2OS cell line, which contains a functional p53 response to DNA damage [24] such as that caused by etoposide. Surprisingly, soluble γH2AX levels were increased fourfold in coilin siRNA compared to control siRNA transfected cells treated with etoposide (Fig. 1). A similar increase in γH2AX levels has been observed upon

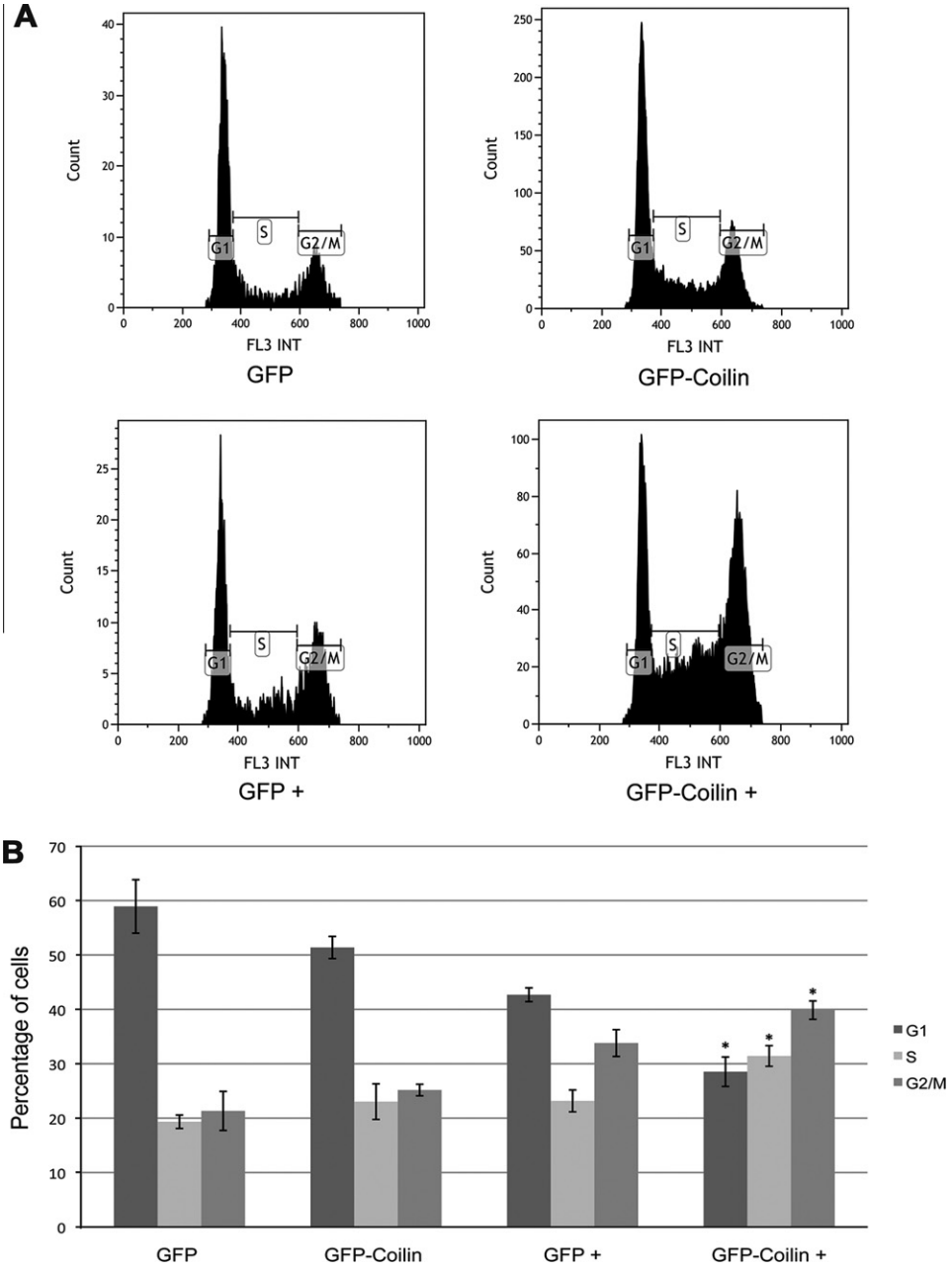

Fig. 3. Transiently transfected coilin increases the percent of cells in S and G2/M after etoposide treatment. (A) U2OS cells expressing GFP or GFP-coilin were untreated or subjected to etoposide treatment (+) 24 h after transfection, followed by FACS analysis. Cell cycle distribution was conducted only on cells expressing GFP or GFP-coilin. (B) The bar graph represents the mean percentage of each cell cycle phase ± standard error about the mean from three independently conducted experiments. * = $p < 0.05$ versus G1, S and G2/M phases of treated GFP expressing cells.

reduction of peroxiredoxin V (PrxV), which is an antioxidant protein that partially accumulates in CBs [25]. The role of chromatin-associated γH2AX in orchestrating the DNA repair proteins at the site of DNA damage is well-established [26–29]. In contrast, soluble γH2AX function is less well understood, but is reported to have pro-apoptotic properties [24]. Since coilin reduction increased the amount of soluble γH2AX in etoposide treated cells, we suspect that coilin negatively regulates the production of γH2AX and/or positively regulates the factors that subsequently acetylate and ubiquitinate γH2AX. Thus, when coilin is reduced, the level of soluble γH2AX is increased. It is important to note that coilin does not accumulate at sites of DNA damage, nor does coilin depletion alter the number of γH2AX repair foci (analyzed at 3 and 16 hrs post-etoposide treatment) or level of DNA damage as accessed via comet assay (our unpublished results). These findings indicate that coilin impacts soluble γH2AX levels, but does not participate in its initial formation. The exact mechanism(s) leading to the release of γH2AX from damaged chromatin is unknown. However, it is known that γH2AX must be acetylated prior to ubiquitination by the TIP60-UBC13 complex, which leads to the release of γH2AX from chromatin [30]. Future studies will more clearly elucidate the mechanism by which DNA damage induces soluble γH2AX, and the role of coilin in this process.

We show here that coilin knockdown significantly decreased the proliferation rate in untreated U2OS cells (Fig. 2A). These results are in agreement with previous reports showing that coilin knockdown reduces cell viability in HeLa cells [9,10,20,11]. Paradoxically, coilin knockdown significantly attenuates the reduction

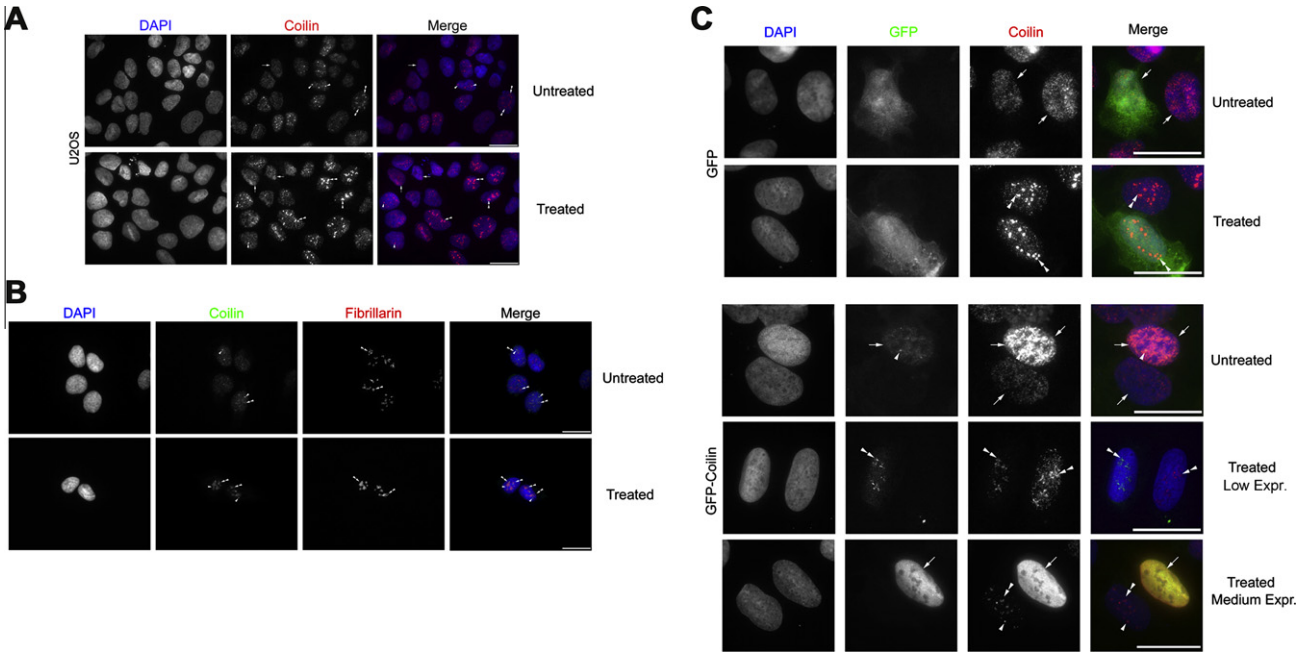

Fig. 4. Coilin levels influence nucleolar accumulation in etoposide treated U2OS cells. (A) Distribution of coilin (red) in untreated and etoposide treated U2OS cells. DAPI staining was used to detect the nucleus (blue). In untreated cells (upper panel), an arrow indicates a cell with nucleoplasmic coilin but lacking CB, arrowheads denote coilin in CBs, and double arrowheads show nucleolar coilin accumulation. In etoposide treated cells, the percent of cells with nucleolar coilin accumulation (double arrowhead) is increased compared to that found in untreated cells. Scale bars = 10 μm. (B) Untreated and etoposide treated U2OS cells were co-stained with antibodies to detect coilin (green) and fibrillarin (red). Double arrowheads mark nucleolar accumulations, and arrowheads indicate CBs. (C) Over expression of GFP-coilin suppresses the nucleolar accumulation of endogenous coilin in etoposide treated U2OS cells. Cells were transfected with GFP or GFP-coilin and 24 h post transfection cells were treated with etoposide or left untreated, and then stained to detect coilin (red) or GFP/GFP-coilin (green). DAPI (blue) was used to detect the nucleus. Arrowheads denote CBs and double arrowheads indicate nucleolar coilin. For untreated cells transfected with the empty GFP vector, arrows indicate two cells, one of which is expressing GFP, which have nucleoplasmic coilin but lack CBs. For untreated cells transfected with GFP-coilin vector, arrows also indicate two cells, one of which is expressing GFP-coilin. Treated cells expressing low and medium levels of GFP-coilin are shown. Scale bars = 10 μm.

of proliferation associated with etoposide treatment. In other words, in the presence of etoposide, coilin knockdown increases cell number over that found with coilin present (Fig. 2A). This same phenomenon has been observed using another type of DNA damaging agent (cisplatin) on other cell lines (HeLa, Saos2 and WI-38) [16]. We speculate that diminished snRNP resources as a consequence of abolished CBs cause the observed decrease in proliferation rate in coilin knockdown untreated cells. In contrast, we hypothesize that cell proliferation is not as drastically reduced in coilin knockdown cells because the nucleoplasmic function of coilin may responsible for the promotion of cell cycle arrest or death in response to DNA damage. Since the normal response for endogenous coilin in the presence of DNA damage induced by etoposide, cisplatin or γ-irradiation is to translocate to the nucleolus (Fig. 4A and B, [16]), we speculate that nucleolar coilin participates in the arrest of the cell cycle, possibly via reduction of snRNP biogenesis and RNA pol I activity, until such time that the DNA has been repaired. We have previously shown that the nucleolar accumulation of coilin caused by another DNA damaging agent (cisplatin) is correlated with reductions in pol I activity [16]. Hence, it is possible that the nucleolar accumulation of coilin as a consequence of etoposide treatment also impacts pol I activity. Alternatively or additionally, we have shown that coilin has in vitro RNA binding and RNase activity [12], thus it is also possible that nucleolar coilin disrupts rRNA processing or stability.

In summary, the data obtained from this and other studies indicate that the localization of coilin may influence cell cycle progression. We hypothesize that coilin in the CB promotes proliferation by ensuring that adequate snRNP resources are present. Although far from proven, we further hypothesize that nucleolar coilin induced by the presence of DNA damaging agents arrests the cell cycle, possibly by inhibiting RNA pol I or rRNA processing. Nucleoplasmic coilin, in contrast, may promote cell death in the presence of DNA damage by inappropriately increasing progression through the cell cycle. Current and future work should more precisely define the role of coilin in this response and clarify the function of coilin in the nucleoplasm, nucleolus and CB.

Acknowledgements

We thank the UMMC Cancer Institute Flow Cytometry Core Facility for FACS analysis. This work was supported by National Institutes of Health grant R01GM081448.

Appendix A. Supplementary data

Supplementary data associated with this article can be found, in the online version, at http://dx.doi.org/10.1016/j.febslet.2012.07.054.

References

[1] Spector, D.L., Lark, G. and Huang, S. (1992) Differences in snRNP localization between transformed and non-transformed cells. Mol. Biol. Cell 3, 555–569.
[2] Gall, J.G. (2000) Cajal bodies: the first 100 years. Annu. Rev, Cell. Dev. Biol. 16, 273–300.
[3] Morris, G.E. (2008) The Cajal body. Biochim. Biophys. Acta 1783, 2108–2115.
[4] Matera, A.G., Izaguire-Sierra, M., Praveen, K. and Rajendra, T.K. (2009) Nuclear bodies: random aggregates of sticky proteins or crucibles of macromolecular assembly? Dev. Cell 17, 639–647.
[5] Strzelecka, M., Oates, A. and Neugebauer, K.M. (2010) Dynamic control of Cajal body number during zebrafish embyogenesis. Nucleus 1 (1), 96–108.
[6] Liu, J.L. et al. (2009) Coilin is essential for Cajal body organization in Drosophila melanogaster. Mol. Biol. Cell 20, 1661–1670.
[7] Tucker, K.E. et al. (2001) Residual Cajal bodies in coilin knockout mice fail to recruit Sm snRNPs and SMN, the spinal muscular atrophy gene product. J. Cell Biol. 154, 293–307.

[8] Walker, M.P., Tian, L. and Matera, A.G. (2009) Reduced viability, fertility and fecundity in mice lacking the cajal body marker protein, coilin. PLoS One 4, e6171.
[9] Lemm, I., Girard, C., Kuhn, A.N., Watkins, N.J., Schneider, M., Bordonne, R. and Luhrmann, R. (2006) Ongoing U snRNP biogenesis is required for the integrity of Cajal bodies. Mol. Biol. Cell 17, 3221–3231.
[10] Whittom, A.A., Xu, H. and Hebert, M.D. (2008) Coilin levels and modifications influence artificial reporter splicing. Cell Mol. Life Sci. 65, 1256–1271.
[11] Hebert, M.D. (2010) Phosphorylation and the Cajal body: modification in search of function. Arch. Biochem. Biophys. 496, 69–76.
[12] Broome, H.J. and Hebert, M.D. (2012) In Vitro RNase and nucleic acid binding activities implicate Coilin in U snRNA processing. PLoS One 7, e36300.
[13] Lyon, C.E., Bohmann, K., Sleeman, J. and Lamond, A.I. (1997) Inhibition of protein dephosphorylation results in the accumulation of splicing snRNPs and coiled bodies within the nucleolus. Exp. Cell Res. 230, 84–93.
[14] Hebert, M.D. and Matera, A.G. (2000) Self-association of coilin reveals a common theme in nuclear body localization. Mol. Biol. Cell 11, 4159–4171.
[15] Hearst, S.M. et al. (2009) Cajal-body formation correlates with differential coilin phosphorylation in primary and transformed cell lines. J. Cell Sci. 122, 1872–1881.
[16] Gilder, A.S., Do, P.M., Carrero, Z.I., Cosman, A.M., Broome, H.J., Velma, V., Martinez, L.A. and Hebert, M.D. (2011) Coilin participates in the suppression of RNA polymerase I in response to cisplatin-induced DNA damage. Mol. Biol. Cell 22, 1070–1079.
[17] Morency, E., Sabra, M., Catez, F., Texier, P. and Lomonte, P. (2007) A novel cell response triggered by interphase centromere structural instability. J. Cell Biol. 177, 757–768.
[18] Cioce, M., Boulon, S., Matera, A.G. and Lamond, A.I. (2006) UV-induced fragmentation of Cajal bodies. J. Cell Biol. 175, 401–413.
[19] Sun, J., Xu, H., Subramony, S.H. and Hebert, M.D. (2005) Interactions between Coilin and PIASy partially link Cajal bodies to PML bodies. J. Cell Sci. 118, 4995–5003.
[20] Toyota, C.G., Davis, M.D., Cosman, A.M. and Hebert, M.D. (2010) Coilin phosphorylation mediates interaction with SMN and SmB'. Chromosoma 119, 205–215.
[21] Xu, Y., Sun, Y., Jiang, X., Ayrapetov, M.K., Moskwa, P., Yang, S., Weinstock, D.M. and Price, B.D. (2010) The p400 ATPase regulates nucleosome stability and chromatin ubiquitination during DNA repair. J. Cell Biol. 191, 31–43.
[22] Velma, V., Carrero, Z.I., Cosman, A.M. and Hebert, M.D. (2010) Coilin interacts with Ku proteins and inhibits in vitro non-homologous DNA end joining. FEBS Lett. 584, 4735–4739.
[23] Gordaliza, M., Garcia, P.A., del Corral, J.M., Castro, M.A. and Gomez-Zurita, M.A. (2004) Podophyllotoxin: distribution, sources, applications and new cytotoxic derivatives. Toxicon 44, 441–459.
[24] Liu, Y., Parry, J.A., Chin, A., Duensing, S. and Duensing, A. (2008) Soluble histone H2AX is induced by DNA replication stress and sensitizes cells to undergo apoptosis. Mol. Cancer 7, 61.
[25] Kropotov, A.V., Grudinkin, P.S., Pleskach, N.M., Gavrilov, B.A., Tomilin, N.V. and Zhivotovsky, B. (2004) Downregulation of peroxiredoxin V stimulates formation of etoposide-induced double-strand DNA breaks. FEBS Lett. 572, 75–79.
[26] Rogakou, E.P., Boon, C., Redon, C. and Bonner, W.M. (1999) Megabase chromatin domains involved in DNA double-strand breaks in vivo. J. Cell Biol. 146, 905–916.
[27] Sedelnikova, O.A., Pilch, D.R., Redon, C. and Bonner, W.M. (2003) Histone H2AX in DNA damage and repair. Cancer Biol. Ther. 2, 233–235.
[28] Celeste, A. et al. (2002) Genomic instability in mice lacking histone H2AX. Science 296, 922–927.
[29] Dickey, J.S., Redon, C.E., Nakamura, A.J., Baird, B.J., Sedelnikova, O.A. and Bonner, W.M. (2009) H2AX: functional roles and potential applications. Chromosoma 118, 683–692.
[30] Ikura, T. et al. (2007) DNA damage-dependent acetylation and ubiquitination of H2AX enhances chromatin dynamics. Mol. Cell Biol. 27, 7028–7040.